Solvent Effect on Redox Properties of Hexanethiolate Monolayer-Protected Gold Nanoclusters

Bin Su,[†] Meiqin Zhang,[‡] Yuanhua Shao,[‡] and Hubert H. Girault*[,†]

Laboratoire d'Electrochimie Physique et Analytique, Ecole Polytechnique Fédérale de Lausanne, Station 6, CH-1015 Lausanne, Switzerland, and Institute of Analytical Chemistry, College of Chemistry and Molecular Engineering, Peking University, 100871 Beijing, China

Received: February 10, 2006; In Final Form: August 17, 2006

The capacitance of monolayer-protected gold nanoclusters (MPCs), C_{MPC}, in solution has been theoretically reconsidered from an electrostatic viewpoint, in which an MPC is considered as an isolated charged sphere within two dielectric layers, the intrinsic coating monolayer, and the bulk solvent. The model predicts that the bulk solvent provides an important contribution to C_{MPC} and influences the redox properties of MPCs. This theoretical prediction is then examined experimentally by comparing the redox properties of MPCs in four organic solvents: 1,2-dichloroethane (DCE), dichloromethane (DCM), chlorobenzene (CB), and toluene (TOL), in all of which MPCs have excellent solubility. Furthermore, this set of organic solvents features a dielectric constant in a range from 10.37 (DCE) to 2.38 (TOL), which is wide enough to probe the solvent effect. In these organic solvents, tetrahexylammonium bis(trifluoromethylsulfonyl)imide ($THATf_2N$) is used as the supporting electrolyte. Cyclic and differential pulse voltammetric results provide concrete evidence that, despite the monolayer protection, the solvent plays a significant effect on the properties of MPCs in solution.

1. Introduction

Nanometer-sized nanoparticles (NPs) are a new class of materials bridging from molecules to bulk materials. The research interest on NPs comes from the fact that they have properties significantly different from those of molecules and bulk materials with the same chemical composition and that these properties are dependent on their size, shape, and surface modification. A spectacular level of research activity has been witnessed in the past decade because of the availability of new synthetic strategies and new techniques for characterization. For example, following the pioneering work by Brust et al.,[1,2] rather stable metallic NPs can be obtained by protecting them with a monolayer of thiol compounds. The NPs prepared with this approach can be isolated and allow further chemical functionalization in order to fulfill various applications.[3] By carefully controlling the reaction conditions, gold NPs with a metallic core containing different numbers of gold atoms can be prepared. This group of NPs is sometimes called monolayer-protected clusters (MPCs),[3] with which the transition from single molecules to bulk materials can be observed.[3,4]

MPCs with metallic core diameters of ∼1.6 nm exhibit at room temperatures the electrochemical behavior of multivalent redox molecules, characterized by a series of redox states regularly spaced along the potential axis.[5] This behavior has been first considered as a quantized property originating from charging the tiny molecular capacitor of MPCs.[5,6] Because the capacitance of an MPC is less than an attofarad (aF), single electron addition to or removal from the tiny MPC capacitor requires a substantial voltage change, which is a property akin to the Coulomb blockade charging. The electrochemistry of MPCs has been extensively studied by several groups.[3−5,7] A series of factors, including the solvent,[8] the temperature,[9] as well as the solvation and/or penetration of solvent and supporting electrolyte,[8,10,11] have been investigated. So far, the model of quantized capacitance charging developed by Murray et al.[6] has been extensively employed to explain the multivalent redox behavior of MPCs. In addition, we have recently proposed another model and calculated the absolute standard redox potentials for MPCs.[12]

The present work aims at understanding the effect of organic solvent on the redox properties of MPCs. The capacitance of an MPC in solution, C_{MPC}, is theoretically reconsidered from an electrostatic viewpoint, which predicts that the solvent outside the MPC sphere generates an important contribution to C_{MPC} and influences the redox properties of MPCs. This prediction is then evaluated experimentally by comparing the electrochemical behavior of MPCs in four organic solvents: 1,2-dichloroethane (DCE), dichloromethane (DCM), chlorobenzene (CB), and toluene (TOL). This set of organic solvents features a relative permittivity in a range from 10.37 (DCE) to 2.38 (TOL).[13] Tetrahexylammonium bis(trifluoromethylsulfonyl)imide ($THATf_2N$) is used as the supporting electrolyte in these solvents. The voltammetric results demonstrate that the average potential separation between neighboring redox waves, ΔV, increases with decreasing the relative permittivity of the solvent. The agreement between the experimental data and the theoretical prediction of the model of absolute standard redox potentials of MPCs is observed, indicating the solvent plays a significant effect on the redox properties of MPCs.

2. Experimental Section

2.1. Chemicals. Hydrogen tetrachloroaurate trihydrate ($HAuCl_4 \cdot 3H_2O$, 99.9%), tetraoctylammonium bromide (TOABr,

* Corresponding author. E-mail: hubert.girault@epfl.ch. Telephone: +41-21 693 3151. Fax: +41-21 693 3667.
[†] Laboratoire d'Electrochimie Physique et Analytique.
[‡] Institute of Analytical Chemistry.

10.1021/jp060874t CCC: $33.50
Published on Web 09/29/2006

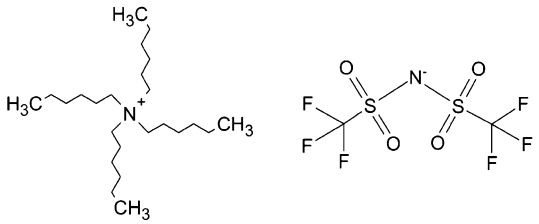

Figure 1. Molecular structure of $THATf_2N$.

98%), and 1-hexanethiol (C_6-SH, 95%) were purchased from Aldrich. Sodium tetrahydroborate ($NaBH_4$, 98%) and lithium bis(trifluoromethylsulfonyl)imide ($LiTf_2N$) were bought from Acros. Ethanol (~96%), acetonitrile (CH_3CN, 99.5%), 1,2-dichloroethane (DCE, ≥99.5%), dichloromethane (DCM, ≥99.5%), chlorobenzene (CB, ≥99.5%), toluene (TOL, ≥99.5%), and tetrahexylammonium chloride (THACl, ≥96.0%) were obtained from Fluka. DCE, DCM, CB, and TOL were dried with molecular sieves before using and all the other chemicals were used as received without further purification.

2.2. Synthesis of MPCs. Hexanethiolate-protected MPCs were prepared by the Brust reaction[1,2] followed by extraction and annealing treatments.[14] Finally, a fraction of MPCs that are ethanol soluble with a mean diameter of 1.6 ± 0.4 nm in the metallic core were obtained as demonstrated previously.[12]

2.3. Synthesis of $THATf_2N$. $THATf_2N$ was prepared by metathesis of THACl and $LiTf_2N$ in a molar ratio of 1:1 in water under vigorous stirring. The reaction was allowed to proceed overnight and resulted in a milky mixture, to which DCM was added. The mixing liquids were further stirred overnight. Then the DCM layer was separated with a separating funnel and the water layer was washed with DCM as described above three times. The DCM solution containing $THATf_2N$ was rotary evaporated to remove DCM. The viscous liquid remaining in the round-bottom flask included $THATf_2N$ and possibly unreacted residues. The obtained ionic liquids were washed with a large amount of ultrapure water and then dried in a vacuum at 100 °C. The molecular structure of $THATf_2N$ is schematically illustrated in Figure 1.

2.4. Electrochemical Measurements. Cyclic voltammetry (CV) and differential pulse voltammetry (DPV) of MPCs in various organic media (ca. 0.08 mM MPC, 0.05 M $THATf_2N$) were performed on a CHI 900 electrochemical workstation (CH Instruments, TX). A two-electrode arrangement was used, in which a silver wire was used both as a quasireference electrode (QRE) and a counter electrode. The working electrode was a 25 μm diameter disk-shaped Pt microelectrode (CH Instruments, TX), which was polished with 0.05 μm Al_2O_3 slurry and then rinsed with water and acetone and dried prior to each measurement. CV was conducted at a scan rate of 0.1 V s^{-1} and DPV was done with a scan rate of 0.02 V s^{-1}, pulse height of 0.1 V, pulse width of 0.05 s, and period of 0.5 s.

3. Results and Discussion

3.1 Reconsideration of the Capacitance of MPCs in Solutions: Electrostatic Model. Considering an MPC as two conducting concentric spheres (CS), its capacitance has been derived by Murray et al.,[6] which is here designated C_{CS} and expressed as:

$$C_{CS} = 4\pi\epsilon_0\epsilon_d\left(\frac{r_0}{d}\right)(r_0 + d) \tag{1}$$

where ϵ_0 is the permittivity of the vacuum and ϵ_d is the relative permittivity of the alkanethiolate protecting monolayer. r_0 and d are the radius of the metallic core and the thickness of the protecting monolayer, respectively. However, it should be clarified that the concentric sphere capacitor model cannot be applied to an MPC. In terms of the basic electrostatic theory, the concentric sphere capacitor consists of two concentric conducting spheres, such as two metallic spheres.[15] Therefore, although an MPC has a concentric structure, a spherical metallic core coated with a uniform dielectric layer, it does not necessarily mean that it can be considered as two concentric conducting spheres. Indeed, the concentric sphere model implies that the electric field is nil outside the protecting monolayer, which is definitely not the case (vide infra). As demonstrated further below, the dielectric medium provides an important contribution to the capacitance of MPCs.

An MPC is by nature an isolated sphere with an intrinsic dielectric layer. In solutions, the situation is that of a charged metallic core surrounded by two dielectric layers, the intrinsic protecting layer and the medium outside. The capacitance of an MPC can be readily obtained from Gauss's theorem by evaluating its electrostatic potential. By applying Gauss' law to the metallic core, the electric field outside inside and outside the protecting layer is:

$$E(r) = \frac{q}{4\pi\epsilon_0\epsilon_d r^2} \qquad (r_0 \le r \le r_0 + d) \tag{2}$$

$$E(r) = \frac{q}{4\pi\epsilon_0\epsilon_s r^2} \qquad (r_0 + d \le r < \infty) \tag{3}$$

where q is the charge that the metallic core carries and ϵ_s is the relative permittivity of the medium outside the MPC sphere. Thus, the potential of the charged core corresponds to the integration the electric field from infinity to the core:

$$\begin{aligned} V &= \int_{r_0}^{\infty} E(r)\,\mathrm{d}r \\ &= \frac{q}{4\pi\epsilon_0}\left(\int_{r_0+d}^{\infty}\frac{\mathrm{d}r}{\epsilon_s r^2} + \int_{r_0}^{r_0+d}\frac{\mathrm{d}r}{\epsilon_d r^2}\right) \\ &= \frac{q}{4\pi\epsilon_0}\left[\frac{d}{\epsilon_d r_0(r_0+d)} + \frac{1}{\epsilon_s(r_0+d)}\right] \end{aligned} \tag{4}$$

Then, from the definition of the capacitance, the capacitance of an MPC, C_{MPC}, is:

$$C_{MPC} = \frac{q}{V} = 4\pi\epsilon_0\epsilon_d\epsilon_s r_0\left(\frac{r_0 + d}{\epsilon_s d + \epsilon_d r_0}\right) \tag{5}$$

This equation clearly differs from that previously reported by Murray et al., given by eq 1. To verify the validity of eq 5, we can consider the limiting conditions. Taking $d \to \infty$ and $d \to 0$ gives $C_{MPC} = 4\pi\epsilon_0\epsilon_d r_0$ and $C_{MPC} = 4\pi\epsilon_0\epsilon_s r_0$, which correspond to the capacitance of MPCs in bulk media of relative permittivity ϵ_d and ϵ_s, respectively. Equation 1 in fact is a limiting case of eq 5 by assuming $\epsilon_s \to \infty$. Therefore, eq 5 represents the precise electrostatic equation describing the capacitance of an MPC embedded in a dielectric medium from an electrostatic viewpoint.

Alternatively, C_{MPC} can also be defined as the sum of two capacitance in series corresponding to the protecting monolayer capacitance, C_{PM}, and the bulk solvent capacitance, C_{BS}:

$$\frac{1}{C_{MPC}} = \frac{1}{C_{PM}} + \frac{1}{C_{BS}} \tag{6}$$

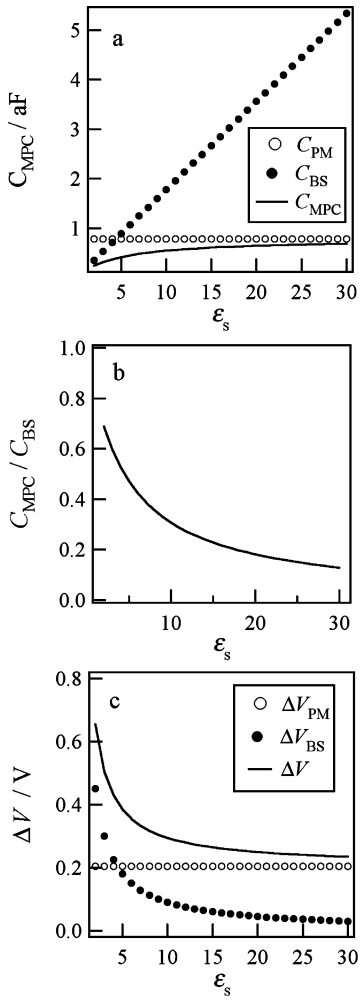

Figure 2. (a) Magnitudes of C_{MPC}, C_{PM}, and C_{BS} calculated from eqs 6, 7, and 8; (b) estimation of the contribution of C_{BS} to C_{MPC} in terms of eq 9; (c) calculated ΔV_{PM}, ΔV_{BS}, and ΔV as a function of ϵ_s according to eqs 7, 8, and 10. The parameters are used as follows: $\epsilon_d = 4.436$, $r_0 = 0.8$ nm, $d = 0.8$ nm.

with C_{PM} and C_{BS} being expressed, respectively, by:

$$C_{PM} = 4\pi\epsilon_0\epsilon_d\left(\frac{r_0}{d}\right)(r_0 + d) \tag{7}$$

$$C_{BS} = 4\pi\epsilon_0\epsilon_s(r_0 + d) \tag{8}$$

The magnitudes of C_{MPC}, C_{PM}, and C_{BS} calculated from eqs 6, 7, and 8 are displayed in Figure 2a. It can be seen that C_{PM} is an intrinsic property of the MPC and represents the capacitance resulting from the protecting monolayer, which is calculated to be 0.78 aF by taking $r_0 = d = 0.8$ nm and $\epsilon_d = 4.436$.[16] C_{BS} is proportional to ϵ_s.

We can see that, if C_{PM} is significantly smaller than C_{BS}, it becomes the predominant factor. This can be evaluated by the contribution of C_{BS} to C_{MPC}:

$$\frac{C_{MPC}}{C_{BS}} = \frac{\epsilon_d r_0}{\epsilon_s d + \epsilon_d r_0} \tag{9}$$

As illustrated in Figure 2b, the contribution of C_{BS} to C_{MPC} continuously increases with decreasing the dielectric constant of the medium, from ~10% at $\epsilon_s = 30$ to ~70% at $\epsilon_s = 2$. Considering the electrochemical measurements reported are performed usually in organic media with ϵ_s around 10, this contribution will be 30−40%, which means that the solvent has a strong effect on the capacitance value of the MPCs and cannot be neglected. Furthermore, in terms of eq 6, the successive single electron charging the metal core of an MPC occurs with a voltage separation:

$$\begin{aligned}\Delta V = \frac{e}{C_{MPC}} &= \frac{e}{C_{PM}} + \frac{e}{C_{BS}} \\ &= \Delta V_{PM} + \Delta V_{BS} \\ &= \frac{e}{4\pi\epsilon_0(r_0 + d)}\left(\frac{d}{\epsilon_d r_0} + \frac{1}{\epsilon_s}\right)\end{aligned} \tag{10}$$

where e is the elementary charge. ΔV_{PM} and ΔV_{BS} represent the potential drops in the protecting monolayer and the bulk solvent, respectively. Taking $C_{PM} = 0.78$ aF as estimated above, ΔV_{PM} is equal to 0.20 V and is determined only by the geometry of the MPC. On the other hand, eq 10 predicts that ΔV increases with decreasing the relative permittivity of the medium. As shown in Figure 2c, the contribution of ΔV_{BS} to the total value increases with decreasing the relative permittivity of the medium. When ϵ_s is less than 10, that is, in usual organic solvents, ΔV_{BS} is comparable to ΔV_{PM}. Therefore, in usual organic solvents used previously, the effect of solvent on the properties of MPCs cannot be ignored.

Furthermore, as demonstrated previously, on the basis of a thermodynamic cycle and the Born's model of ionic solvation, the absolute standard redox potentials of freely diffusing MPCs in solutions can be formulated and are given in a form:[12]

$$[E^0_{Z/Z-1}]_{abs} = \frac{\Phi_b}{e} + \frac{\left(z - \frac{1}{2}\right)e}{4\pi\epsilon_0(r_0 + d)}\left(\frac{d}{\epsilon_d r_0} + \frac{1}{\epsilon_s}\right) \tag{11}$$

where Φ_b is the work function of the metal. The voltage separation between successive single electron-transfer events produced by eq 11 is therefore:

$$\Delta V = \frac{e}{4\pi\epsilon_0(r_0 + d)}\left(\frac{d}{\epsilon_d r_0} + \frac{1}{\epsilon_s}\right) = \frac{e}{C_{MPC}} \tag{12}$$

By comparing eqs 10 and 12, it can be seen that these two approaches are self-consistent, yielding the same expression for the voltage separation. This is due to the fact that both approaches treat the solvent as a dielectric continuum.

3.2. The Capacitance of MPCs in Electrolyte Solutions: Electrical Double-Layer Model. In the presence of ions in solutions, an MPC can be considered as a nanoelectrode with an electric double layer consisting of a compact layer and a diffuse layer.[9−11] The total potential drop across the MPC/electrolyte interface corresponds to the sum of the potential drops in two layers:

$$\phi^M - \phi^S = (\phi^M - \phi^2) + (\phi^2 - \phi^S) \tag{13}$$

or

$$\Delta V = \Delta V_{COM} + \Delta V_{DL} \tag{14}$$

where ϕ^2 expresses the potential at the distance r_2 from the MPC center. ϕ^2 in fact represents the potential at the boundary between the compact layer and the diffuse layer. Differentiating eqs 14 or 15 with respect to the charge gives the double-layer capacitance at the MPC/electrolyte interface, which is also designated C_{MPC} and can be represented as a compact layer

capacitance (C_{COM}) and a diffuse layer capacitance (C_{DL}) in series:

$$\frac{1}{C_{MPC}} = \frac{1}{C_{COM}} + \frac{1}{C_{DL}} \tag{15}$$

The diffuse layer can be considered in terms of the classical Gouy−Chapman theory. However, two points are worth discussing to use this theory. First, the parameter r_2, which in principle represents the inner-layer thickness determined by the closest approach of the diffuse-layer ions, is difficult to assign. Second, treating the diffuse layer around a spherical nanoparticle is not a simple matter, and one often needs elaborate numerical methods[10] or to take certain approximations. For example, Murray et al. has used the planar Gouy−Chapman theory, considering the diffuse layer around a nanoparticle as that of a planar electrode.[9,11] This simplified approach can yield, using the Debye−Hückel approximation, a potential distribution in the diffuse layer:

$$\phi(r) = \frac{q}{4\pi {r_2}^2 \epsilon_0 \epsilon_s \kappa} e^{-\kappa(r-r_2)} \tag{16}$$

with κ being the reciprocal Debye length:

$$\kappa = \sqrt{\frac{2e^2 n^0}{\epsilon_0 \epsilon_s kT}} \tag{17}$$

in the case of 1:1 electrolyte ions. n^0 is the volumic density of ions in the bulk. If considering the spherical coordinates, the electrical potential distribution around a charged particle is given by:[17]

$$\phi(r) = \frac{q}{4\pi\epsilon_0\epsilon_s}\left(\frac{e^{\kappa r_2}}{1+\kappa r_2}\right)\left(\frac{e^{-\kappa r}}{r}\right) \tag{18}$$

If assuming $r_2 = r_0 + d$, we have $C_{COM} = C_{PM}$ and $\Delta V_{COM} = \Delta V_{PM}$, and the planar and spherical diffuse layer capacitances derived from eqs 16 and 18 are:

$$C_{DLP} = C_{BS}[\kappa(r_0 + d)] \tag{19}$$

$$C_{DLS} = C_{BS}[1 + \kappa(r_0 + d)] \tag{20}$$

In eqs 19 and 20, the term in brackets represents the ionic contribution to the capacitance and C_{BS} represents the bulk solvent contribution. In most experimental conditions, $[\kappa(r_0 + d)]$ is larger than 1, and therefore, the two equations become equivalent. Furthermore, in the planar and spherical approximations, the single electron charging the MPC capacitor occurs with a voltage separation, respectively:

$$\Delta V_{Planar} = \Delta V_{PM} + \Delta V_{DLP} = \frac{e}{C_{PM}} + \frac{e}{C_{BS}[\kappa(r_0 + d)]} \tag{21}$$

$$\Delta V_{Spherical} = \Delta V_{PM} + \Delta V_{DLS} = \frac{e}{C_{PM}} + \frac{e}{C_{BS}[1 + \kappa(r_0 + d)]} \tag{22}$$

From eqs 21 and 22, we can examine how the voltage of single electron charging changes with the dielectric property of the medium. Figure 3a shows the evolution of ΔV_{DLP} and ΔV_{DLS} with ϵ_s, both increasing slowly with decreasing ϵ_s. The difference between ΔV_{DLS} and ΔV_{DLP} is not large. However, ΔV_{DLP} and ΔV_{DLS} are much smaller than ΔV_{PM}. Therefore, the total potential separation is largely determined by ΔV_{PM}, and ΔV values calculated from eqs 21 and 22 remain much smaller than those experimentally observed, as shown in Figure 3b and further below in Figure 7a.

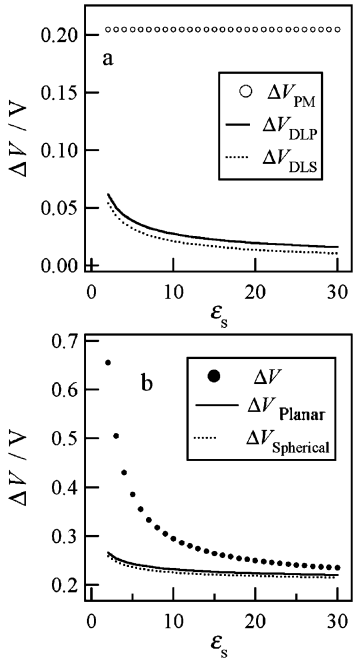

Figure 3. (a) Calculated ΔV_{PM} and ΔV_{DLP} and ΔV_{DLS} as a function of ϵ_s according to eqs 7, 19−22; (b) total potential separations, ΔV_{Planar} and $\Delta V_{Spherical}$, as a function of ϵ_s in terms of eqs 21 and 22. ΔV calculated from eq 10 is also compared. The parameters are used as follows: $\epsilon_d = 4.436$, $r_0 = 0.8$ nm, $d = 0.8$ nm, $n^0 = 3.011 \times 10^{25}$ m^{-3} ($c^0 = 0.05$ M), $T = 298.15$ K.

3.3. Solvent Effect on Redox Properties of MPCs. As a matter of fact, both experimental and theoretical investigations of the solvent effect on redox properties of MPCs have been carried out previously.[11,12] In a very early work, it has been concluded that the redox properties of MPCs were not sensitive to the solvent relative permittivity.[8] This conclusion was supported by the experimental measurements in various organic solvents or mixed organic solvents with a relative permittivity over a range of nearly 3-fold from 14.1 to 5.53, in which the ΔV value was reported to be relatively constant. In contrast, recently, by changing the relative permittivity of the mixed solvents by varying the ratio of two component solvents, it has been reported that the solvent has a strong effect on redox behavior of MPCs.[11] The effect was ascribed to the complicated specific solvation and/or penetration of the alkanethiolate monolayer by the less polar solvent and supporting electrolyte ions in the mixed solvents. However, it is important to note that these measurements were carried out in mixed solvents. To a certain extent, the comparative analysis of previous results would be difficult to perform precisely on account of the indeterminate physicochemical properties of mixed solvents.

The choice of solvent for electrochemical measurements is determined by the consideration of the joint solubility of the MPCs and the supporting electrolyte. Table 1 lists four types of organic solvents, 1,2-dichloroethane (DCE), dichloromethane (DCM), chlorobenzene (CB), and toluene (TOL), in all of which MPCs have rather good solubility. On the other hand, this set of organic solvents features a relative permittivity ranging from 10.37 (DCE) to 2.38 (TOL),[13] which is wide enough to probe the solvent effect on the redox properties of MPCs according to eq 10. The viscosities of the organic solvents are also compared in Table 1. $THATf_2N$, which is a type of room

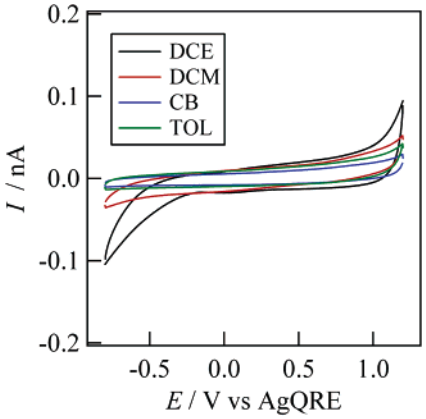

Figure 4. Potential windows obtained on a 25 μm microelectrode in four organic solvents with 0.05 M $THATf_2N$ as supporting electrolytes. The scan rate is 0.1 V s^{-1} in all cases.

TABLE 1: Electrochemical Measurements in Various Solvents

solvent	abbreviated symbol	relative permittivity (ϵ_s)	viscosity (mPa s)
1, 2-dichloroethane	DCE	10.37	0.779
1, 2-dichloromethane	DCM	8.93	0.413
chlorobenzene	CB	5.69	0.753
toluene	TOL	2.38	0.560

temperature ionic liquid and exhibits excellent solubility in the four organic solvents, was used as the common supporting electrolyte. It should be mentioned that the electrochemical measurements at room temperatures in a single TOL phase has been previously hindered by the lack of supporting electrolyte. Recently, it has been demonstrated that $THATf_2N$ can be employed as a supporting electrolyte in TOL, providing sufficient conductivity for electrochemical measurements.[18] Figure 4 displays the potential windows in four organic media obtained on a 25 μm microelectrode with 0.05 M $THATf_2N$ as supporting electrolyte. Apparently, a potential window ranging from −0.8 to 1.2 V could be easily attained in each solvent. The cathodic and anodic current onsets observed at the end of the potential window can be related to the reduction of oxygen and the oxidation of H_2O, respectively. H_2O may come from either the organic solvent or $THATf_2N$. Please note that removal of water from ionic liquids is very difficult. By degassing the solution with nitrogen or argon gas, a potential window with a much more negative limiting potential can be obtained in each organic solution. Beyond all doubt, Figure 4 clearly shows the applicability of $THATf_2N$ as the common supporting electrolyte in four solvents.

Figure 5 shows the CVs of 0.08 mM MPCs in four solvents with 0.05 M $THATf_2N$ as the supporting electrolyte. It is obvious that each CV is characteristic of a certain number of well-defined steady-state current−potential waves typically observed on a microelectrode. These waves result from successive redox reactions involving MPCs, which provide clear evidence that MPCs can be considered as multivalent redox species. Most importantly, the solvent effect on the redox properties of MPCs can be observed from Figure 5. From DCE to TOL, the number of current−potential waves in the same potential window continuously decreases while ΔV increases, which will be discussed below in more detail. Moreover, these waves are well separated from each other along the potential axis and can be analyzed individually. For a disk microelectrode, the diffusion-controlled limiting current is proportional to the radius of microelectrode (a), the diffusion coefficient (D), and

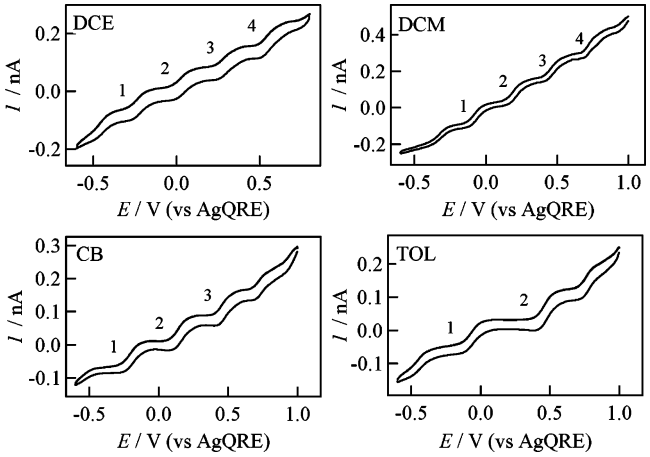

Figure 5. CVs obtained on a 25 μm microelectrode for 0.08 mM MPCs in various solvents with 0.05 M $THATf_2N$ as supporting electrolytes. The scan rate is 0.1 V s^{-1} in all cases. The labeled waves were further analyzed.

TABLE 2: Diffusion Coefficients of MPCs in Various Solvents Calculated from Steady-State Waves Labeled in Figure 5

solvent	wave number	D ($\times 10^{-6}$ cm^2 s^{-1})
DCE	1	1.97
	2	1.86
	3	1.91
	4	2.19
DCM	1	3.10
	2	3.46
	3	3.43
	4	3.69
CB	1	2.00
	2	1.99
	3	1.99
TOL	1	2.08
	2	2.36

the concentration (c) of the redox species:

$$I_s = 4nFDac \tag{23}$$

Therefore, from the microelectrode voltammograms, one can derive the diffusion coefficient of redox species in terms of eq 23. Table 2 displays the diffusion coefficients of MPCs derived from those labeled waves observed in various organic solvents. In one solvent, the values of D do not vary much with the charge states of MPCs, which means that the MPC charge does not materially affect its diffusion rate. In general, the values of D are within a range of $2.0-4.0 \times 10^{-6}$ cm^2 s^{-1}, which is in good agreement with those reported previously.[14] Considering the average values of diffusion coefficients in DCE, DCM, CB, and TOL, a ratio of $D_{DCE}:D_{DCM}:D_{CB}:D_{TOL} = 1.0:1.7:1.0:1.1$ can be attained. On the other hand, in terms of the classical Stokes−Einstein equation, the diffusion coefficient of a spherical object is proportional to the reciprocal of the solvent viscosity:

$$D = \frac{K}{\eta} \tag{24}$$

where η is the solution viscosity and K is a parameter consisting of the Boltzmann constant, the temperature, and the hydrodynamic radius of MPCs. On the basis of eq 24, the ratio of diffusion coefficient of MPCs in various solvents is also in good agreement with the reciprocal ratio of the solvent viscosity, which is $1/\eta_{DCE}:1/\eta_{DCM}:1/\eta_{CB}:1/\eta_{TOL} = 1.0:1.9:1.0:1.4$.

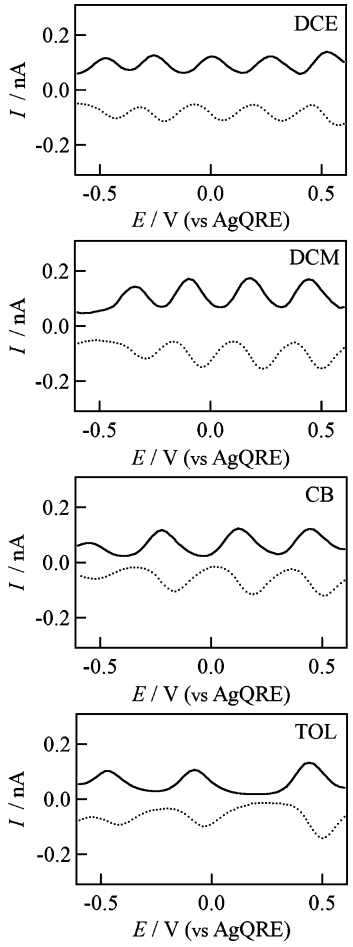

Figure 6. DPVs (solid: anodic scan; dotted: cathodic scan) of 0.08 mM MPCs in various solvents with 0.05 M $THATf_2N$ as supporting electrolytes: scan rate 0.02 V s^{-1}, pulse height 0.1 V, pulse width 0.05 s, and period 0.5 s.

As shown above in Figure 5, the number of steady-state waves in the same potential window decreases with decreasing the relative permittivity of organic solvent, which indicates the strong effect of solvent on the redox properties of MPCs. This can be seen much more clearly by DPV measurements. The DPV responses of MPCs change with the organic solvent in two aspects. First, as shown in Figure 6, in a potential window ranging from −0.6 to 0.6 V, the number of observed current peaks decreases from 5 in DCE to 4 in DCM and CB and to 3 in TOL. In DCE, DCM, and CB, the observed current peaks are very similar and uniformly spaced along the potential axis, with the average peak separation, ΔV, increasing with decreasing the relative permittivity of organic solvents. Second, the irregular distribution of current peaks is observed in the whole potential range in TOL, where ΔV value declines continuously by increasing of the applied voltage with a large separation of 0.53 V between the second and the third peaked currents. In fact, the irregular distribution of current peaks was also observed in the high potential regime in CB (not shown here).

The increase of ΔV with decreasing the relative permittivity is in agreement with the prediction of eq 10. This tendency can be clearly seen from Figure 7a, in which ΔV values of the neighboring current peaks in each organic solvent are displayed. The horizontal axis in Figure 7a, $n_{\text{peak separation}}$, has nothing to do with the real charge state of MPCs. This number is used just for simplicity and $n_{\text{peak separation}} = 1$ represents the potential separation of the first and second current peaks on the left side in Figure 6. It is clearly demonstrated in Figure 7a that ΔV

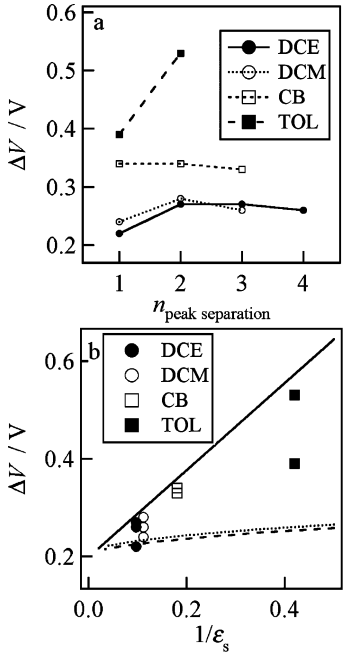

Figure 7. (a) Illustration of potential separations of current peaks observed in Figure 6; (b) dependence of ΔV on the reciprocal of the solvent relative permittivity. The solid, dotted, and dashed traces correspond to the theoretical curves of eqs 10, 21, and 22, respectively, using parameters as in Figure 3.

increases when decreasing the relative permittivity of the organic solvent. In DCE and DCM, the difference in ΔV is not so big, as theoretically, it is only about 10 mV according to eq 10. But the increase in ΔV is much more clearly observed when MPCs are dissolved in CB. These experimental observations provide concrete evidence that the organic solvent has significant effect on the redox properties of MPCs in it.

The relation of the peak separations versus the reciprocal of the solvent relative permittivity is further plotted, as displayed in Figure 7b. The solid, dotted, and dashed lines correspond to the theoretical curves of eqs 10, 21, and 22, respectively, with $r_0 = d = 0.8$ nm, $\epsilon_d = 4.436$,[16] $z = 1$, $n^0 = 3.011 \times 10^{25}$ m^{-3} (assuming the absence of ion pair formation), and $T = 298.15$ K. It can be seen that most data points are close to the theoretical curve of eq 10 except the first ΔV value in TOL. However, it should be mentioned that all the current peaks observed in TOL are irregularly spaced. Admittedly, the redox behavior of MPCs in TOL is more complicated and difficult to analyze than that in other solvents. Generally speaking, from Figure 7a, the agreement between the experimental phenomenon and the theoretical prediction of eq 10 can be observed, which verifies that despite the monolayer protection the solvent still has a significant effect on the redox properties of MPCs in solutions. The experimental data corroborate a solvent continuum model of the absolute standard redox potential of MPCs.[12]

On the other hand, the distribution of ΔV in the high potential regime in CB and in the whole potential range in TOL becomes irregular, which can be rationalized by different approaches. First, this irregular spacing can be attributed to the activity coefficient of the MPC, which affects the formal redox potential

$$E^0_{Z/Z-1}{}' \left(E^0_{Z/Z-1}{}' = E^0_{Z/Z-1} + \frac{RT}{F} \ln\left(\frac{\gamma_{MPC^Z}}{\gamma_{MPC^{Z-1}}}\right)\right)$$

Indeed, the activity coefficient of the MPC should vary with its charge as predicted by the Debye−Hückel theory and therefore results in a variation of the formal redox potential.[17]

Second, it may be ascribed to the effects of solvent penetration in the protecting monolayer and electrolyte ion binding. The solvent penetration in the MPC-protecting monolayer can change the values of ϵ_d and d significantly. For example, it has been reported that toluene can penetrate strongly into the alkanethiolate-protecting monolayer of gold nanoparticles, inducing the alkyl chains to spread out from the gold nanoparticles.[19] The binding of electrolyte ions to MPC sphere can also shift the redox potential of MPCs if the binding process is considered as a chemical reaction coupled to the MPC redox reaction. Further investigations on the boundary between the protecting monolayer and the solvent will be helpful in understanding the properties of MPCs. A third possible explanation for the irregular distribution of ΔV may reflect the real distribution of populated electronic states within the Au core, which are not regularly distributed as assumed but do appear regularly in a certain dielectric medium or in a certain potential range.

Acknowledgment. This work is partly supported by grants from EPFL and the Fonds National Suisse de la Recherche Scientifique (200020-105486). M. Zhang and Y. Shao gratefully acknowledge the financial support from the National Natural Science Foundation of China (20420130137, 20475003, and 20235010). Technical assistance by Valerie Devaud is also acknowledged.

References and Notes

(1) Brust, M.; Fink, J.; Bethell, D.; Schiffrin, D. J.; Kiely, C. *J. Chem. Soc., Chem. Commun.* **1995**, 1655−1656.

(2) Brust, M.; Walker, M.; Bethell, D.; Schiffrin, D. J.; Whyman, R. *J. Chem. Soc., Chem. Commun.* **1994**, 801−802.

(3) Templeton, A. C.; Wuelfing, W. P.; Murray, R. W. *Acc. Chem. Res.* **2000**, *33*, 27−36.

(4) Chen, S. *J. Electroanal. Chem.* **2004**, *574*, 153−165.

(5) Chen, S.; Ingrma, R. S.; Hostetler, M. J.; Pietron, J. J.; Murray, R. W.; Schaaff, T. G.; Khoury, J. T.; Alvarez, M. M.; Whetten, R. L. *Science* **1998**, *280*, 2098−2101.

(6) Chen, S.; Murray, R. W.; Feldberg, S. W. *J. Phys. Chem. B* **1998**, *102*, 9898−9907.

(7) Ingram, R. S.; Hostetler, M. J.; Murray, R. W.; Schaaff, T. G.; Khoury, J.; Whetten, R. L.; Bigioni, T. P.; Guthrie, D. K.; First, P. N. *J. Am. Chem. Soc.* **1997**, *119*, 9279−9280.

(8) Hicks, J. F.; Templeton, A. C.; Chen, S.; Sheran, K. M.; Jasti, R.; Murray, R. W.; Debord, J.; Schaaff, T. G.; Whetten, R. L. *Anal. Chem.* **1999**, *71*, 3703−3711.

(9) Miles, D. T.; Murray, R. W. *Anal. Chem.* **2003**, *75*, 1251−1257.

(10) Quinn, B. M.; Liljeroth, P.; Ruiz, V.; Laaksonen, T.; Kontturi, K. *J. Am. Chem. Soc.* **2003**, *125*, 6644−6645.

(11) Guo, R.; Georganopoulou, D.; Feldberg, S. W.; Donkers, R.; Murray, R. W. *Anal. Chem.* **2005**, *77*, 2662−2669.

(12) Su, B.; Girault, H. H. *J. Phys. Chem. B* **2005**, *109*, 11427−11431.

(13) Izutsu, K. *Electrochemistry of Nonaqueous Solutions*; Wiley-VCH: New York, 2002.

(14) Hicks, J. F.; Miles, D. T.; Murray, R. W. *J. Am. Chem. Soc.* **2002**, *124*, 13322−13328.

(15) Taylor, D. M.; Secker, P. E. *Industrial Electrostatics: Fundamentals and Measurements*; Research Studies Press Ltd.: Somerset: U.K., 1994.

(16) Lide, D. R., Ed. *CRC Handbook of Chemistry and Physics*, 86th ed.; CRC Press: Boca Raton, FL, 2005−2006.

(17) Girault, H. H. *Analytical and Physical Electrochemistry*; EPFL Press: Lausanne, Switzerland, 2004.

(18) Zhang, M.; Liu, H.; Hu, H.; Xie, S.; Jing, P.; Li, M.; Gan, L.; Kou, Y.; Shao, Y. 2006, submitted.

(19) Pei, L.; Mori, K.; Adachi, M. *Colloids Surf., A* **2006**, *281*, 44−50.